SLAC-PUB-11702
February 2006
(A)

The S-Band 1.6 Cell RF Gun Correlated Energy Spread Dependence on π and 0 Mode Relative Amplitude*

J. F. SCHMERGE, J. CASTRO, J. E. CLENDENIN, D. H. DOWELL, S. M. GIERMAN AND H. LOOS

SLAC, Stanford University, 2575 Sand Hill Rd
Menlo Park, CA 94025, USA

Abstract

The π mode or accelerating mode in a 1.6 cell rf gun is normally the only mode considered in rf gun simulations. However, due to the finite Q there is a small but measurable 0 mode present even at steady state. The π mode by definition has a 180°phase shift between cells but this phase shift for the total field is several degrees different. This results in a correlated energy spread exiting the gun. A comparison of simulation and experiment will be shown.

Contributed to the workshop on
The Physics and Applications of High Brightness Electron Beams 2005
October 9-14, 2005, Erice, Sicily, Italy

* Work supported by Department of Energy contract DE-AC02-76SF00515.

THE S-BAND 1.6 CELL RF GUN CORRELATED ENERGY SPREAD DEPENDENCE ON π AND 0 MODE RELATIVE AMPLITUDE

J.F SCHMERGE, J. CASTRO, J.E. CLENDENIN, D.H. DOWELL, S.M. GIERMAN AND H. LOOS

SLAC, Stanford University, 2575 Sand Hill Rd
Menlo Park, CA 94025, USA

The π mode or accelerating mode in a 1.6 cell rf gun is normally the only mode considered in rf gun simulations. However, due to the finite Q there is a small but measurable 0 mode present even at steady state. The π mode by definition has a 180°phase shift between cells but this phase shift for the total field is several degrees different. This results in a correlated energy spread exiting the gun. A comparison of simulation and experiment will be shown.

1. Motivation

1.1. *Introduction*

Longitudinal phase space measurements performed at the SLAC Gun Test Facility (GTF) have shown a large correlated energy spread exiting the gun not predicted by simulations[1]. Previous simulations only include the π mode which is the dominant rf mode in the 1.6 cell gun. However, due to the finite Q there is a small but non-zero component of the 0 mode present in the gun at steady state. The total field has phase shift between cells that is approximately 7° off the 180° for a pure π mode case. The phase shift produces a correlated energy spread at the gun exit. This paper describes frequency domain measurements on the gun to characterize the π and 0 mode components as well as comparison of the measured longitudinal phase space with simulations including the 0 mode.

The phase shift of the total field with respect to the π mode also must be accounted for when measuring the phase in the rf gun. Typically the gun phase is determined by measuring the emitted charge as a function of phase[2]. The 0° phase point is defined as the phase where the gun starts to emit. This phase is measured with respect to the total field but is often used in the simulation as the phase with respect to the π mode. For the GTF gun the phase offset between the total field and the π mode in the half cell is approximately 5°.

1.2. *Phase Space Measurements*

Longitudinal phase space is measured at the GTF by measuring the energy spectrum as a function of linac phase[1]. The total energy is measured simultaneously with energy spread in order to determine the absolute phase. Maximum energy is defined as the 0° reference point. Figure 1 shows the results of a typical measurement and the resulting phase space distribution for a charge of 15 pC and a peak current of approximately 10 A. The longitudinal Twiss parameters can be determined at the linac entrance by fitting the measured energy spread as a function of linac phase just as the transverse Twiss parameters are determined from fitting measured beam sizes as a function of quadrupole focal length. Alternatively the measured energy spectrum can be fit using tomographic reconstruction to determine the actual phase space distribution[3].

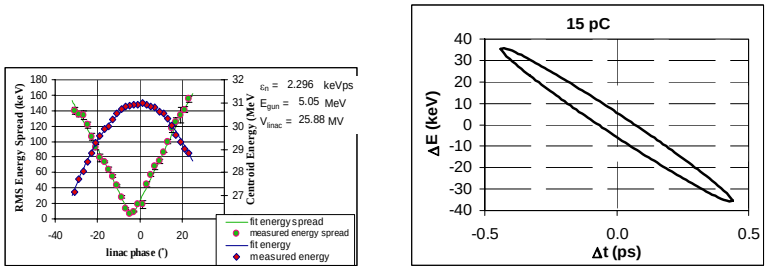

Figure 1. Measured energy and energy spread is plotted on the left along with the fit. The phase is defined to be 0 at the maximum energy. The Twiss parameters from the fit can be used to generate the rms phase space ellipse plotted on the right. This is the distribution approximately 75 cm downstream of the gun at the linac entrance. The beam is chirped with approximately -80 keV/ps.

The measured rms energy spread at the linac entrance is 36 keV while the simulation predicts approximately 10 keV when the applied rf field consists of only the π mode. The energy spread is clearly dominated by the correlated energy spread. The source of this chirp must either be an applied time varying field or a beam induced field. While the chirp does depend on charge a substantial chirp is present at all charges indicating one component of the source must be an applied field. The only applied fields between the cathode and the linac are the rf field in the gun and the DC magnetic field from an emittance compensating solenoid. Thus the rf field is the only time dependent field that could produce the measured chirp shown in figure 1.

Thermionic rf guns produce chirped beams as shown in figure 1 by using a ratio of full cell to half cell fields greater than one[4]. The field ratio was measured to be approximately one during cold testing of the GTF gun prior to

installation. It was theorized that the gun tuning may have changed during multiple cathode changes or that the gun field distribution varied as the rf power was increased. Thus the gun was removed and carefully characterized.

2. Gun Characterization

Initially the gun had a single rf probe monitoring the field outside the full cell. The rf probe is a coaxial line with the center conductor extended past the outer conductor. The full cell had two identical holes located 180° apart one of which was used for the rf waveguide feed and the second was used as a vacuum pump out port. The probe is located in the pump out section. A second probe monitoring the half cell field was added outside one of the two laser ports. Each probe has a different response due to the different field strength at the probe position. The probe response was assumed independent of frequency over the few MHz range of the experiment. A cross section of the rf gun showing the location of the two probes is shown in Figure 2.

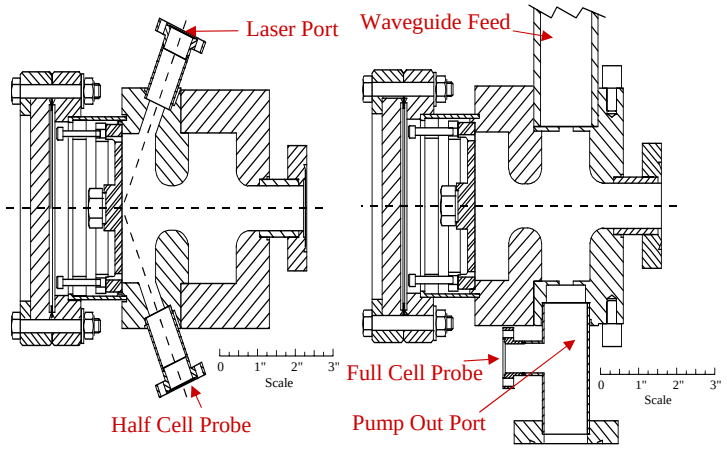

Figure 2. A cross section of the 1.6 cell photo-cathode gun is shown. The figure on the left shows the two grazing incidence laser ports, one of which was used to install an rf probe. The figure on the right is rotated 45° about the beam axis with respect to the first figure and it shows the waveguide feed and pump out port. The full cell probe is located in the pump out port region.

The gun was characterized in the frequency domain using a network analyzer with port 1 connected to the waveguide feed and port 2 to either the full cell or half cell probe. The measured transmission normalized amplitude and phase is plotted in Figure 3 for both probes. The constant and linear terms of the measured phase were modified to correct the phase reference point of the

network analyzer and path length differences. Figure 3 shows the mode at 2856 MHz has a 180° phase shift between cells while the remaining mode has a 0° phase shift. These are by definition the π and 0 modes respectively.

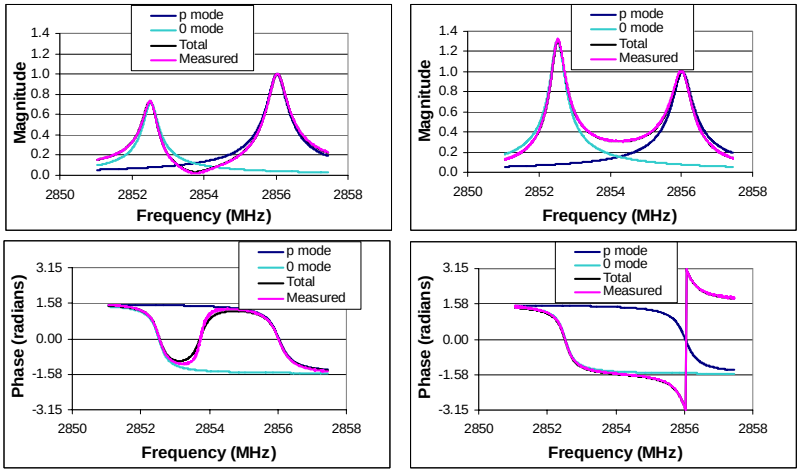

Figure 3. The S_{12} parameter normalized amplitude and phase with port 2 connected to the full cell on the left and the half cell on the right. The measured field is plotted in red and the fit in black. The fit is composed of two second order bandpass filters which are plotted in blue and turquoise.

A model of the two cell gun composed of two bandpass filters was used to fit the data with a least square error fitting routine. The frequency response of the model is given in equation 1 where f_{rf}, f_π and f_0 are the excitation frequency, the π mode frequency and the 0 mode frequency respectively. Q_π and Q_0 are the loaded Qs and A_π and A_0 are the normalized mode amplitude which depends on z. The model parameters fit to the data are listed in Table 1. The time constant for each mode is defined in equation 2. The reflection data or S_{11} parameter was also measured to determine the rf coupling coefficient β.

$$A_{ss}e^{j\theta_{ss}}\left(f_{rf},z\right)=\left[\frac{jA_\pi\left(z\right)\frac{f_\pi}{Q_\pi}f_{rf}}{f_\pi^2-f_{rf}^2+j\frac{f_\pi}{Q_\pi}f_{rf}}+\frac{jA_0\left(z\right)\frac{f_0}{Q_0}f_{rf}}{f_0^2-f_{rf}^2+j\frac{f_0}{Q_0}f_{rf}}\right] \quad (1)$$

$$\tau_{\pi,0}=\frac{Q_{\pi,0}}{\pi f_{\pi,0}} \quad (2)$$

Due to the different probe responses, the frequency response measurement can not determine the ratio of the field in the full cell to the half cell. A bead drop measurement was used to determine the field amplitude versus position. The bead data indicate the π mode has a full cell to half cell field ratio of 1 ± 0.02 and is used to set the normalized amplitude of the π mode in the full and half cell to +1 and -1 respectively. With this definition of normalized field, the probe response is -44.1 dB for the full cell probe and -53.0 dB for the half cell probe.

Table 1. The measured rf parameters for the π and 0 mode.

Parameter	π mode	0 mode
$A_{(full\ cell)}$	+1	+0.72
$A_{(half\ cell)}$	-1	+1.31
f_0 (MHz)	2856.03	2852.53
Q	5160	6980
β	1.34	0.68
τ (ns)	576	779

After characterization the gun was re-installed and operated. The rf probes were used to measure the field in each cell at full power. Figure 4 shows the measured fields in each cell as a function of time. Approximately 6 MW of power is required to reach a field of 90 MV/m in the gun. As the plot indicates the ratio of the field is roughly independent of time. The time shift between the two probe signals is due to cable length differences.

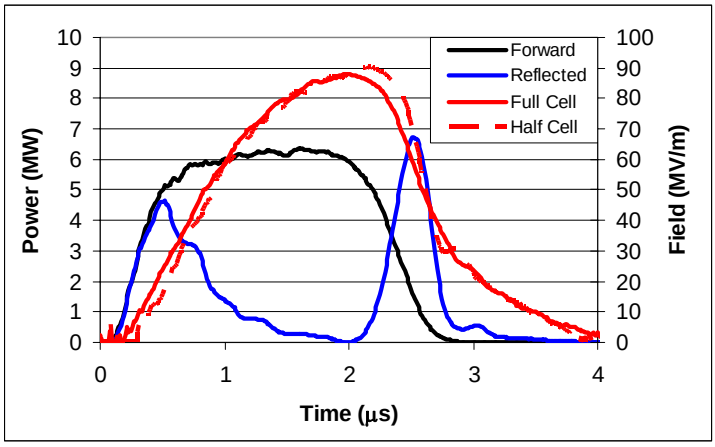

Figure 4. The measured amplitude of the full cell and half cell probes along with the incident and reflected rf power signals. The data was collected using a crystal detector.

The peak field measured by the two probes agrees to within approximately 2%. Thus the on axis field at full power and low power are identical and a field ratio >1 is not the source of the correlated energy spread.

3. 0 Mode Contribution

Next, the 0 mode component of the total field was studied to determine if it could produce a correlated energy spread. The total field in the gun is given by the sum of the fields from the two modes. The total field can be calculated from the model parameters listed in table 1. For a step function excitation the field is given in equation 3. A_{ss} and θ_{ss} are the steady state amplitude and phase from equation 1. The effect of the two transient terms are assumed small due to the exponential decay and are not considered in this paper.

$$V(t) = A_{ss}\cos\left(\omega_{RF}t + \theta_{ss}\right) + B_{\pi}e^{-\frac{t}{\tau_{\pi}}}\cos\left(\omega_{\pi}t + \phi_{\pi}\right) + B_{0}e^{-\frac{t}{\tau_{0}}}\cos\left(\omega_{0}t + \phi_{0}\right) \quad (3)$$

The relative amplitude and phase for each mode in each cell has been computed and is listed in table 2 for an excitation frequency of 2856.00 MHz. Since the 0 mode is nearly 90° out of phase with the π mode, the total field amplitude is approximately equal to the π mode amplitude but the total field phase is changed by several degrees. The effect is greatest in the half cell where the 0 mode amplitude is the largest. The phase advance between cells is nearly 7° larger for the total field than the π mode alone.

Table 2. The calculated amplitude and phase for the π , 0 mode and total field in both the full and half cell. The phase is measured with respect to the incident field.

Field	Full Cell	Half Cell
π mode	1∠0°	1∠180°
0 mode	0.044∠-86.7°	0.076∠-86.7°
Total ($A_{ss}\angle\theta_{ss}$)	1.003∠-2.5°	0.998∠184.4°

Figure 5 is a GPT simulation of the energy spread as a function of linac phase where the results of four different simulations are shown demonstrating the effect on the energy spread due to both the 0 mode and space charge. The green curve is a simulation excluding both the 0 mode and space charge. Including the 0 mode but not space charge results in the blue curve. This shifts the curve closer to the experimental data but it still does not reproduce the experimental results. The pink curve includes space charge but not the 0 mode and once again it does not match the experimental results. The red curve

includes the 0 mode and space charge and actually matches the experiment fairly well. However, in order to get good agreement with the experiment the 0 mode amplitude in the half cell was increased to 12% of the π mode instead of the measured 8% and the laser phase was reduced to 20° with respect to the π mode field instead of the measured 24°. The discrepancy may be due to the presence of transient field components and measurements are in progress to determine the contribution of the transient rf fields to the correlated energy spread. The results indicate space charge does contribute to the correlated energy spread. Both space charge and the 0 mode must be included in the simulations even at the relatively low peak current of 10 A in order to reasonably reproduce the experimental results.

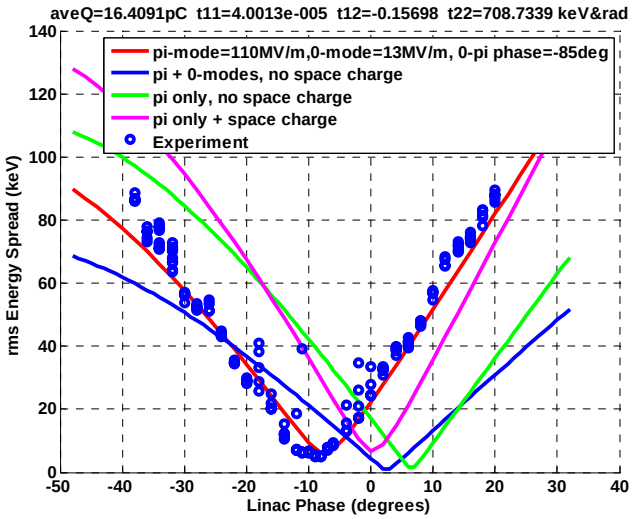

Figure 5. The measured energy spread versus linac phase is plotted as open circles along with the results of four GPT simulations. The green curve is the result of the simulation with the 0 mode and space charge excluded. The blue curve includes the 0 mode but not space charge and the pink curve includes space charge but not the 0. The red curve includes both space charge and the 0 mode.

4. Conclusions

A large correlated energy spread is produced at the gun exit. The correlated energy spread is not due to a full cell to half cell field ratio greater than one.

The field ratio was measured to be nearly one at both low power with a bead drop and at full power with calibrated field probes in each cell.

A model of the two cell gun was fit to the frequency domain measurements. Based on the fit parameters the steady state field due to the π and 0 modes could be computed along with the total field. The total field has a phase advance between cells of 187° instead of the 180° degrees for the π mode. Also, in the half cell the phase difference between the π mode and the total field is approximately 5°. Measurements of the laser phase determine the phase of the laser with respect to the total field and not the π mode. The correct laser phase must be included in the simulation to predict the correct energy spread.

Simulations using the code GPT show that both space charge and the 0 mode contribute to the correlated energy spread. The simulation can reproduce the experimental results but it requires a 0 mode amplitude larger than is measured. The best agreement with the measured data occurs with a 0 mode amplitude 12% of the π mode amplitude instead of the measured 8% and a laser phase of 20° instead of the measured 25°. The discrepancy might be due to the transient rf field contribution and is currently under investigation.

Simulations should include the 0 mode component of the gun field in order to accurately compute the longitudinal phase space. The non-zero component of the 0 mode at the cell to cell iris may also contribute to the transverse emittance. The LCLS gun is designed with a mode separation of 15 MHz instead of 3.5 MHz as in the GTF gun. Thus the LCLS gun will have a phase advance between cells of 181°. The 0 mode contribution is significantly suppressed with the larger mode separation and the adverse beam effects will not be present.

Acknowledgments

This work supported by the U.S. Department of Energy under contract number DE-AC02-76SF00515.

References

1. D.H. Dowell et al, “Longitudinal emittance measurements at the SLAC gun test facility”, NIM Vol A507, pp. 331-334, 2003.
2. J.F. Schmerge et al, “RF gun photo-emission model for metal cathodes including time dependent emission”, to be published in these Proceedings.
3. H. Loos, et al, “Longitudinal phase space tomography at the SLAC gun test facility and the BNL DUV-FEL ”, NIM Vol A528, pp. 189-193, 2004.
4. M. Borland, “A high-brightness thermionic microwave electron gun”, SLAC Report 402, 1991. http://www.slac.stanford.edu/pubs/slacreports/slac-r-402.html